CCFE
CULHAM CENTRE FOR FUSION ENERGY

UK Atomic Energy Authority

UKAEA-CCFE-PR(25)321

Lawrence Shere, Niklas Beere, Rosemary Brown,
Rachel Lawless, Timothy J. Mays, Semali P. Perera,
Alfred K. Hill

Hydrogen Isotope Separation in "Trapdoor" Chabazite as Measured by a Novel Breakthrough Sonic Gas Sensor

Hydrogen Isotope Separation in “Trapdoor” Chabazite as Measured by a Novel Breakthrough Sonic Gas Sensor

Lawrence Shere, Niklas Beere, Rosemary Brown, Rachel Lawless,
Timothy J. Mays, Semali P. Perera, Alfred K. Hill

This is a preprint of a paper submitted for publication in
International Journal of Hydrogen Energy

Hydrogen Isotope Separation in “Trapdoor” Chabazite as Measured by a Novel Breakthrough Sonic Gas Sensor

Lawrence Shere [a], Niklas Beere [a], Rosemary Brown [b], Rachel Lawless[b], Timothy J. Mays[a], Semali P. Perera [a], and Alfred K. Hill [a*]

[a] Department of Chemical Engineering, University of Bath, Bath BA2 7AY, UK

[b] Culham Science Centre, Abingdon, OX14 3DB

* Corresponding author. E-mail address: a.k.hill@bath.ac.uk , Tel: +44 (0) 1225 386486

Highlights

- H_2 and D_2 adsorption/desorption isotherms are presented for potassium chabazite, zeolite 5A and zeolite 3A, HKUST-1 and MOF-74(Ni) between 77 – 273 K. Frontal and displacement breakthrough adsorption experiments are presented for the first time for sodium-potassium chabazite and zeolite 5A.
- Potassium chabazite is shown to selectively block H_2 between 143 – 195 K with an ideal D_2/H_2 selectivity of 1.83 at 143 K.
- Mixed ion sodium-potassium chabazite is shown to have a trapdoor effect with a higher optimal temperature and greater separation factor which is observed to increase further under competitive adsorption compared to single gas isotherms.
- Zeolite 3A is shown to exhibit the trapdoor phenomenon.
- A bespoke whistle gas density sensor shown to measure H_2 and D_2 composition shown to be a cost-effective method for measurement of gas composition.
-
-

Keywords: H_2 isotherms; chabazite; zeolites; Hydrogen isotope separation; Trapdoor mechanism

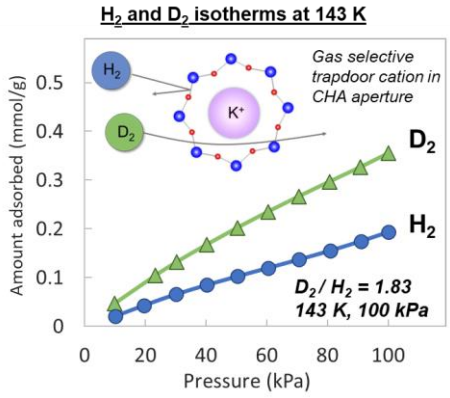

Abstract

Clean energy from nuclear fusion requires the development of an efficient technology for hydrogen isotope separation capable of high separation efficiency with lower energy costs and lower tritium inventory. Isotope separation using adsorbents such as zeolites and MOFs shows great promise due to their high isotope selectivity, but are limited to very low temperatures (<100 K), making them less practical for fusion applications. In this paper, the hydrogen isotope selectivity of 'trapdoor' chabazite is measured for the first time, and shown to be able to operate at relatively mild temperatures, with high selectivity.

Using H_2 and D_2 isotherm measurements, it was observed that at temperatures between 143-195 K, the trapdoor mechanism was able to block H_2 and permit D_2 adsorption in potassium chabazite (K-CHA) and sodium/potassium chabazite (NaK-CHA) leading to high ideal isotope selectivity (D_2/H_2 = 1.83 at 143 K, 100 kPa). Zeolite 5A, zeolite 3A, HKUST-1 and MOF-74(Ni) adsorbents were also tested using H_2 and D_2 isotherms. Evidence is presented for the first time of hysteresis in the trapdoor chabazites and this is also observed for the first time in zeolite 3A, in which it is postulated that a trapdoor effect is also in evidence.

An innovative adsorption breakthrough setup was developed to measure D_2/H_2 separation factor of sodium/potassium chabazite (NaK-CHA) and zeolite 5A under industrially relevant conditions. To provide online measurements of deuterium in hydrogen, a bespoke whistle gas density sensor was successfully tested and used in the setup. The D_2/H_2 separation factor of Na-K chabazite from frontal breakthrough was measured to be 2.71 ± 0.70 at 159 K, much higher than for zeolite 5A at 1.25 ± 0.24 at 159 K and 1.7 ± 0.2 at 77 K. These results show for the first time that efficient hydrogen isotope separation can be achieved in chabazite adsorbents at relatively mild temperatures.

1. Introduction

Fusion is expected to be an important future energy source, providing zero carbon energy generation [1, 2]. However, a number of technical challenges must be solved before fusion power generation can be commercialised. One of these is the requirement of a hydrogen isotope separation technology that must have combined high separation efficiency, low energy

intensity and low tritium inventory. Isotope separation is necessary to produce the 50:50 mixture of deuterium (D_2) and tritium (T_2) fuel and recycle it, since fusion reactors are expected to have a very low burn-up rate of roughly 2% [3, 4]. For a proposed future power plant with 2 GW fusion power, 0.32 kg/day of tritium will be consumed [5] but due to the low burn-up rate the throughput for reprocessing will be 16 kg/day, which is almost 1000 times greater tritium throughput than any current tritium project or ITER which is currently under construction [3, 6]. Conventional hydrogen isotope separation used Cryogenic Distillation for high concentrations of tritium since it has a moderate isotope selectivity (H_2/D_2 separation factor of 2.3 at 24 K [7]), and many stages can be incorporated into a reasonably sized column. However cryogenic distillation requires extremely low operating temperatures (20–24 K), which result in poor energy efficiency and has high tritium inventory in the liquid phase. As a result, no current technology meets the three key performance goals needed for future fusion energy plants.

In recent years, nanoporous adsorbents such as zeolites and metal-organic frameworks (MOFs) have been shown to have a high hydrogen isotope selectivity due to an effect known as Quantum Sieving (QS). Cu(I) open metal sites, such as Cu(I)-MFU-4l, have been reported to have the highest heat of adsorption for hydrogen (32 kJ/mol) [8] leading to high D_2/H_2 selectivity of 11 at relatively high temperatures (100 K). Among the materials with lower heat of adsorption, Bezverkhyy *et al.* [9] recently reported a very high selectivity of 25.8 for chabazite zeolite at 38 K. Most adsorbents require extreme cryogenic operating temperatures (<77 K) and this will increase operation costs and complexity. Furthermore, the low temperature and high heat of adsorption would likely require the use of thermal desorption to fully regenerate the adsorbent after each adsorption cycle – a slow and energy intensive process given the high heat capacity and poor thermal conductivity of these sorbents. Therefore, an adsorbent that could operate at more mild temperatures with high hydrogen isotope selectivity would be more practical for tritium separation applications.

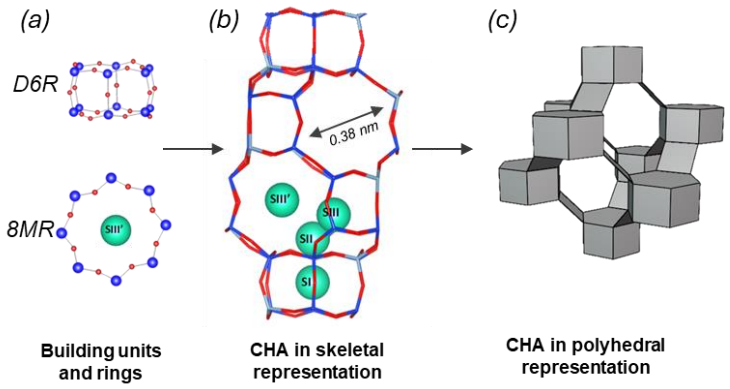

Figure 1 – (a) Building units and rings for chabazite zeolite (CHA)(b) Framework structure and assignment of cation positions for CHA (adapted from [10]). SIII' position in the 8-membered ring (8MR) is favoured by large cations (K^+) which then act as trapdoor cations. (c) polyhedral representation of CHA highlighting passages available to gas molecules (H_2O or larger, including H_2 and D_2) and the chabazite super-cavity accessed through the 8MRs

This paper reports the hydrogen isotope selectivity of chabazite zeolite adsorbent, which utilizes a molecular "trapdoor" mechanism to separate hydrogen isotopes. The "trapdoor" mechanism in CHA has so far been demonstrated to be able to distinguish non-polar gases such as N_2 and CH_4 with high selectivity [11]. The chabazite (CHA) framework contains large super-cavities accessed through narrow 8-membered ring (8MR) apertures of 0.38 nm size [12]. The 8MR aperture is preferentially occupied by large cations such as potassium which can control gas adsorption by acting as "gatekeeping" cations, also referred to as "trapdoor" cations. These gases demonstrate a critical admission temperature, below which the gas is blocked by the gatekeeping cation and adsorption is inhibited. Li *et al.* [13] measured the critical admission temperature for H_2 which was reported to occur at approximately 170 K; much lower than any other non-polar gases such as N_2. Since the critical admission temperature is dependent on the gas type, by selecting a suitable temperature, the trapdoor effect can block one gas type while allowing another to adsorb. If the critical admission temperature is different for H_2 and D_2, the trapdoor effect could be used to separate hydrogen isotopes at temperatures much higher than other adsorbents.

There are no reported D_2 adsorption isotherms or quantitative separation data for hydrogen isotopes using trapdoor CHA but a possible selectivity is indicated by two previous studies. Physick et al. conducted H_2 and D_2 adsorption of Cs exchanged CHA at 293 K using a column breakthrough setup, reporting an isotope selectivity due to a trapdoor admission, but did not provide quantitative adsorption data or separation factor. Taguchi et al. tested K exchanged CHA using Thermal Adsorption Spectroscopy reported an isotope selectivity occurring at ~200 K. However, the separation factor was not reported and the stated H_2 uptake was very low. It remains to be discovered whether a trapdoor chabazite can indeed achieve high separation factors for hydrogen isotope separations with significant uptake, and the nature of the relationship between the trapdoor blocking mechanism and temperature must be better understood.

In this work, H_2 and D_2 isotherm measurements are conducted between 77 – 273 K to find the critical admission temperature of H_2 and D_2 of K-CHA. These isotherm measurements provide understanding of the adsorption equilibria are an important first step in understanding the selectivity of an adsorbent. A thorough comparison of the selectivity performance of the trapdoor effect is made by testing other high performance adsorbents including zeolite 5A, 3A, MOF-74(Ni) and HKUST-1. Breakthrough experiments using mixed D_2/H_2 are then used directly to measure the D_2/H_2 selectivity of NaK-CHA under dynamic adsorption conditions.

Normally, mass spectrometry is required for D_2/H_2 breakthrough testing to provide real time isotope measurements but mass spectrometry is expensive and so is a barrier to these experiment. In this work, a novel sonic gas density detector using a miniaturised whistle was developed, and used successfully to conduct breakthrough testing. Whistle detectors have previously been trialled in Gas Chromatography [14] and more complex sonic standing wave gas density devices [15]. These are the first tests of a whistle type detectors for analysing hydrogen isotopes. This sonic system has the potential to be the first cost-effective and simple alternative to conventional mass spectroscopy for isotope measurements, enabling further research into this important area for fusion energy.

2. Method

Copper nitrate trihydrate (ACS reagent, >97%), nickel acetate tetrahydrate (purum p.a., >99%), potassium hydroxide pellets (ACS reagent), trimesic acid (>95%, benzene-1,3,5-tricarboxylic acid (BTC)), formic acid (ACS reagent, >95%), hydroquinone (reagent plus, >99%), potassium carbonate (ACS reagent, >99%), 37% hydrochloric acid, sodium sulfite (Na_2SO_3, ACS reagent, >98%) were purchased from Merck and used as supplied.

Zeolite 5A powder was purchased from Molsiv Adsorbents, UOP and used as purchased. Zeolite 5A, 1.56 mm pellets were purchased from BDG Chemicals Ltd, Poole, UK and used as supplied. Reagent grade KCl and NaCl were purchased from Sigma Aldrich. Wyoming sodium bentonite was purchased from RS Minerals, UK.

Wyoming sodium bentonite from RS Minerals. Ethanol (>99%), acetone (>99 %) and n-pentane (>99 %) was purchased from VWR and used as supplied.

2.1 Chabazite synthesis using inter-zeolite conversion

Chabazites (CHA) were synthesised from Zeolite Y material using a standard procedure adapted from Gaffney [173] (for the full method, see supporting information).

2.3 Preparation of NaK-CHA pellets

NaK-CHA pellets were prepared bound using 15 wt.% bentonite clay as the binder. A soft paste was formed by adding water and then was extruded through a 2 mm syringe to form pellets. The pellets were fired at 600 °C and ion exchanged using a mixed solution of sodium and potassium salts. The full method can be found in the supporting information.

2.4 Powder X-ray Diffraction (P-XRD)

Powder X-ray Diffraction (P-XRD) was conducted on all samples to identify the presence of high purity crystalline phases. For all samples, the system used was the STOE STADI P which was accessed through the Material and Chemical Characterisation (MC2) laboratory located at the University of Bath. The system is equipped with a Multi-Mythen moving detector and a germanium primary beam monochromator operating in transmission mode using CuKα1 radiation (λ = 1.54051 Å).

2.5 Energy-dispersive X-ray Spectroscopy (EDX)

Energy-dispersive X-ray Spectroscopy (EDX) was used to measure the elemental composition of the prepared CHA to determine the Si/Al ratio and cation content. An Oxford instruments ULTIM max 170 and 10 kV acceleration voltage was used. The powder sample was deposited on carbon tape, and five areas of the sample of roughly 100 µm size were analysed. The error of EDX can be as low as 2 % of the true value [16]. Carbon tape was detected in some EDX tests. However, the carbon tape contains negligible amounts of the elements being analysed.

2.6 Adsorption Isotherms

A Micromeritics 3Flex instrument was used to conduct adsorption and partial desorption isotherms using either H_2, D_2 or N_2. The samples were prepared by initially rough degassed under N_2 flow for 1 h at 90 °C and then at 350°C for 1 h. The samples were then degassed under vacuum at 350 °C for 12 h. Approximately 250 – 350 mg of sample was used for each test. The free space of the sample tube was minimised using a glass filler rod (the same rod in each test) and the free space was directly measured at the end of each experiment using He gas.

During the isotherm measurement, standard temperatures were maintained using liquid nitrogen (77 K) or water ice bath (273 K). Other non-standard isotherm temperatures were achieved using partially frozen cryogenic solvents (pentane – 143 K, ethanol – 159 K, acetone – 178 K, acetone/dry ice – 195 K) and a novel setup using a hanging solvent ice container. Pure solvents have a defined melting point so are ideal for maintaining certain cryogenic temperatures. However, the use of solvent ice normally introduces problems since the solvent ice sinks in the solvent liquid, meaning the top of the Dewar is not directly cooled by the ice and warming at the top causes the free space volume to change. Additionally, large chunks of ice at the bottom could damage the sample tube as it is lowered in. To overcome these issues, a novel setup was used, involving a long container of solvent ice (or dry ice pellets in a mesh cage) suspended in the Dewar next to the sample tube (see Figure 2). This allowed significantly more solvent ice to be packed into the Dewar and helped to prevent warming of the top of the Dewar. A custom-built stainless steel cylindrical mesh cage (30 mm OD, 200 mm high) wrapped in aluminium foil was used as the container.

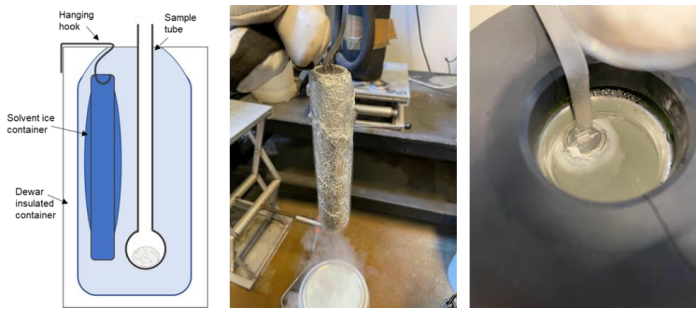

Figure 2: Novel setup of solvent cooling bath used to maintain temperatures for adsorption isotherms. Diagram (right), hanging solvent ice container (centre), hanger placed into Dewar, ready for experiment (right) [Equipment designed and commissioned by the author]

BET surface area was calculated from N_2 isotherms conducted at 77 K. The BET model was fitted to 5 pressure data points in a pressure range for which the value of v_{ads} (1- P/P_0) was always increasing with P/P_o [17]. Pore volume was calculated from the adsorbed amount of N_2 close to saturation pressure at P/P_o = 0.9 and assuming the adsorbed layer has the same density as liquid nitrogen (0.806 g/mol).

Ideal Adsorbed Solution Theory (IAST) was used to calculate the ideal selectivity from the individual H_2 and D_2 isotherms at 77 K. For the high temperature isotherms (143 – 273 K), the isotherm shape is close to linear and so the D_2/H_2 adsorption ratio was used directly as the ideal selectivity.

2.7 Breakthrough rig design and dynamic H_2/D_2 adsorption testing

Breakthrough testing is used to understand the dynamic adsorption of sorbents in columns. The breakthrough rig was designed and constructed as shown in the setup schematic in Figure 3. The experiment was designed to avoid the need for inert gases such as helium, which is becoming a scarce worldwide resource and could interfere with both the adsorption process and gas detection system. Flow rates of between 35.5 – 336 ml_n/min were used with D_2 concentrations between 5 – 28.6 vol%. Normal volumetric gas flow units are used throughout

(reference gas volumetric flow at 273 K and 101.3 kPa with gas molar volume of 22.4 ml_n/mmol). The adsorption column was a u-shaped with 10 mm ID columns and 70 mm length. Please see supporting information for details of column, piping and gas flow controllers.

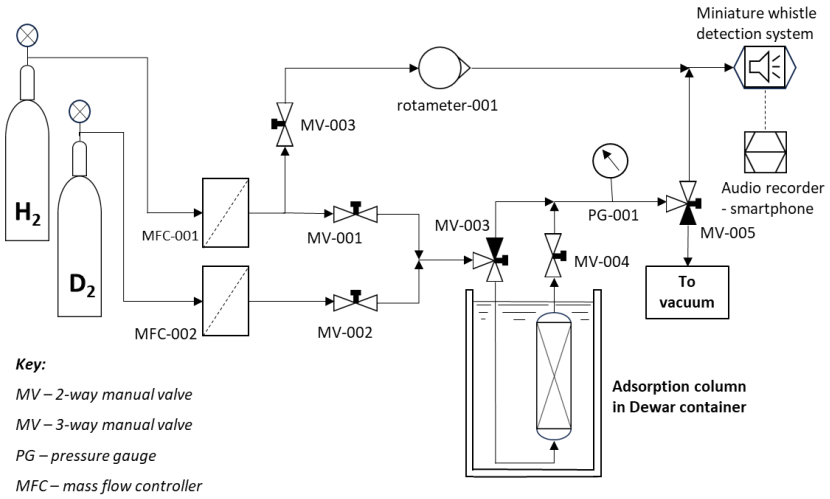

Figure 3: Schematic of breakthrough rig which was designed and constructed for use in dynamic D_2/H_2 adsorption tests using displacement and frontal modes.

The adsorbent samples were degassed in-situ. The adsorption column was heated using two temperature-controlled heating mantles and sand as a heat transfer medium. The samples were firstly degassed under H_2 flow (60 ml_n/min), and the temperature slowly increased to 90 °C and held for 2 hours. The column was then held under vacuum using a diaphragm pump with H_2 flow continued. For zeolite 5A and NaK-CHA, the column was heated to 350 °C and kept at this temperature for 8 hours. For MOF-74(Ni) the temperature was gradually increased by 30 °C every 0.5 h to 250 °C and this temperature was maintained for 8 h.

The adsorbents were tested using two different breakthrough experiments: displacement and frontal breakthrough. For the displacement mode breakthrough test, the adsorption column was firstly saturated with H_2 at 1 bar. The H_2 flow was then switched to mixed D_2/H_2 flow and the time taken for the D_2 to reach the column outlet was measured. See supporting information for full method. In the frontal mode breakthrough test, the adsorption column was initially at vacuum pressure. A flow of mixed D_2/H_2 was introduced at the column inlet (with the outlet closed) to pressurise the column. Once the pressure reaches 1 bar, the outlet was opened, and the composition at the outlet was measured.

2.8 Real-time gas analysis using a bespoke online whistle gas density sensor

An essential part of the breakthrough apparatus for testing mixed D_2/H_2 was a system for isotope detection. The only conventional option for real-time measurement of hydrogen isotopes is Mass Spectrometry but this can be very expensive. A new method for analysing hydrogen isotope composition was tested which was based on the different speed of sound in H_2 and D_2 which causes a change in the sound frequency of a whistle. The whistle was miniaturised, reducing the minimum H_2 flow rate required to produce a stable sound to 336

ml_n/min. Note that the whistle requires turbulent flow to resonate, therefore the minimum flow is likely governed by the Reynolds number. This explains why the minimum flow of hydrogen was much higher than when using air and why using smaller whistle diameters below 1.57 mm did not significantly change the required gas flow.

When the flow to the bed is necessarily lower for lower uptake sorbents, the hydrogen flow was partially bypassed around the bed to maintain the minimum flow to the sensor. In these cases, the deuterium concentration into the bed was increased to maintain the minimum deuterium concentration to the whistle when diluted with the bypassing hydrogen. For these reasons, both the flow rate through the bed and the deuterium concentration to the bed had to be varied depending on the adsorbent and its anticipated uptake.

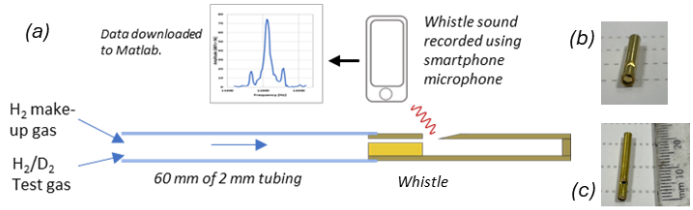

Figure 4: Sonic detection system using a miniaturised whistle to detect changes in the gas density. (a) The whistle required additional gas flow which was provided by a H_2 make-gas line. (b) and (c) photos of the whistle used in the experiments.

The whistle was constructed of a brass tube with an inner diameter of 1.57 mm and total length of 22 mm (15 mm length from edge to back stop). A narrowing in the opening is made by filing a flat edge on a brass rod and this is glued in place (see Figure 4(b). A v-shaped opening was made in the brass tube, just beyond the opening (see Figure 4(c)). The whistle was calibrated against different D_2 concentrations in H_2 and flow rates as shown in the supporting information.

2.9 Breakthrough calculations

The free space of the breakthrough system and column were estimated and corrected for by measurement at 293 K using H_2, (see supporting information for details). The raw signal data was sampled every 3 seconds, and a moving average was applied to remove noise.

Three potential sources of error from each breakthrough experiment were analysed (see supporting information for full analysis): the error in free space correction was found to have negligible impact, manual operation/timing errors contributed 5 – 8%, and error in flow rate supply contributed 5 – 15% of the estimated uptake, largely due to the rotameter instrument, and the combined error was 10 – 23% as a function of flowrate.

Calculation of uptake and selectivity from frontal breakthrough

In the displacement mode breakthrough, the column is initially saturated with H_2. The flow is switched to mixed D_2/H_2 at the start of the experiment. The D_2 displaces the adsorbed H_2, and once the column has reaches maximum D_2 capacity D_2 is detected at the outlet.

The D_2/H_2 separation factor $S(D_2/H_2)$, was calculated from areas (A) and (B) in the frontal breakthrough results, shown in Figure 5 [18]. The free space must be subtracted from area (A) and the units converted to ml_n/(g min) using the flow rate, Q. It is assumed the outlet flow rate is equal to the inlet flow, once the column outlet is opened. Some H_2 adsorption will still be occurring which will reduce the outlet flow. However, this flow effect is minor, and in our setup

the sensor signal responds to this lower flow with lower frequency, and this cancels out this minor effect (see Figure 5).

$$A\ (ml_n/\ (\mathrm{g\ min}) = \frac{A\ (s) \times Q\ (ml_n/\ (\mathrm{g\ min})}{60\ (s/\ \mathrm{min})} - FSV\ (ml_n/g) \quad (2)$$

$$B\ (ml_n/\ (\mathrm{g\ min})) = \frac{B\ (s) \times Q\ (ml_n/\ (\mathrm{g\ min}))}{60\ (s/\ \mathrm{min})} \quad (3)$$

The separation factor was calculated using equation (4):

$$S(D_2/H_2) = \frac{(A+B)}{A} \quad (4)$$

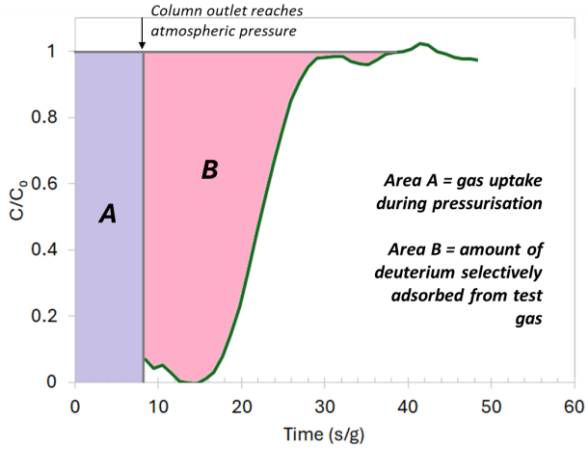

Figure 5: Analysis of frontal mode breakthrough curve. Initially the mixed H_2/D_2 feed is adsorbing to the packing at vacuum pressures with the outlet closed (area a). Next, once the column has reached atmospheric pressure, the outlet is opened and the D_2 concentration is measured. Using areas (a) and (b) the H_2 + D_2 uptake, and D_2/H_2 separation factor can be calculated. Note the breakthrough plot begins above zero. This is because at the beginning, the flow out of the column is lower due to adsorption, and this causes a small reduction in the frequency of the whistle gas density sensor.

The uptake of D_2 and H_2 is calculated from *a* and *b* as follows:

$$uptake\ of\ D_2(ml_n/g) = \ y_D(A + \ B) \quad (5)$$

$$uptake\ of\ H_2(ml_n/g) = \ \mathrm{A}y_H \quad (6)$$

where y_D and y_H are the fractions of D_2 and H_2 in the feed gas respectively ($y_D + y_H = 1$).

3. Results

3.1 Material characterisation

Synthesised K-CHA was tested using powder XRD (see Figure 6) to confirm that the crystal structure of CHA had been produced and that there was no zeolite Y precursor remaining in the sample. Theoretical XRD peaks for CHA occur at 2θ = 9.5, 13, 16, 18, 20.5° while for the zeolite Y precursor they are found at 2θ = 6.2, 10, 12, 15.5, 19° [19].

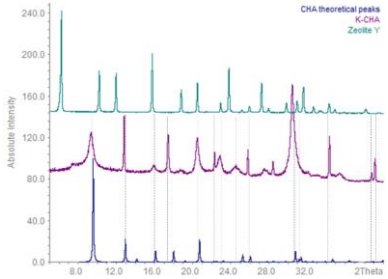

Figure 6: Measured XRD pattern for powdered synthesised CHA (K-CHA) compared against zeolite Y and the theoretical peaks for CHA, confirming CHA has been successfully synthesised with no remaining zeolite Y.

The XRD pattern shows the expected CHA peaks from the theoretical CHA pattern with none of the peaks from Zeolite Y, showing full conversion and a successful synthesis. Some of the K-CHA peaks are slightly shifted and/or wider than the theoretical peaks. Peak broadening is caused by the smaller crystal sizes [12]. The presence of adsorbed water and Al atoms in the framework will shift the peak positions and so will not perfectly conform to the theoretical peaks [12]. The XRD pattern for MOF-74(Ni) and HKUST-1 are shown in the supporting information.

The EDX results showed the K-CHA sample had an Si/Al ratio of 1.98 with a K cation content of 97.6 % with the remainder being Na cations. A N_2 isotherm was conducted at 77 K and the BET surface area was calculated to be 29 m^2/g. This extremely low BET surface area indicates that at the low temperature of 77 K, N_2 is blocked from the pores indicating the presence of a "trapdoor" that is closed for N_2 at 77K. The N_2 isotherms at 77 K for K-CHA, MOF-74(Ni) and HKUST-1 are given in the Supporting Information.

Table 1: Summary of EDX results from testing K-CHA and two ion exchanged CHA samples.

Sample	Ion exchange (mol%)	Cations detected	Si/Al ratio	Cation/Al ratio
K-CHA	97.6 ± 0.4	K, Na	1.98 ± 0.05	1.01 ± 0.10
K-CHA(IE)	98.5 ± 0.01	K, Na	1.92 ± 0.02	0.94 ± 0.08
NaK-CHA	81.8 ± 0.01	K, Na	2.06 ± 0.01	1.01 ± 0.04

3.2 Effect of temperature on H_2 & D_2 adsorption to K-CHA

H_2 and D_2 isotherms were measured for K-CHA at different temperatures between 77 K and 273 K. The amount of H_2 and D_2 adsorbed at 100 kPa for each temperature and the ideal D_2/H_2 selectivity was calculated and is shown in Figure 7 alongside the isotherms curves:

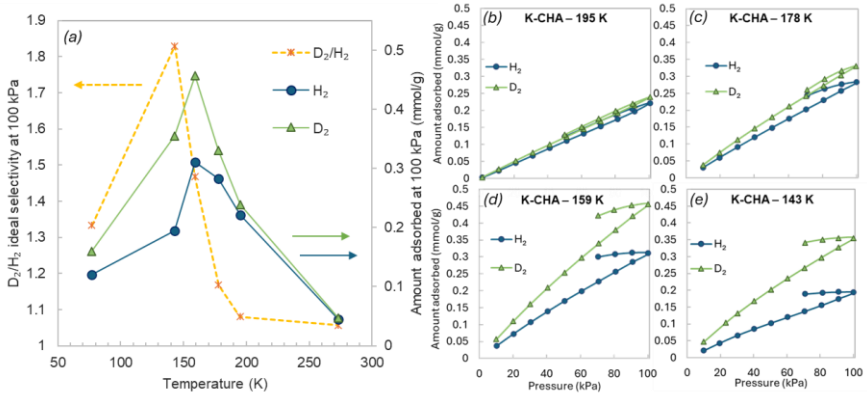

Figure 7: (a) H_2 and D_2 adsorption and ideal D_2/H_2 selectivity of K-CHA at 100 kPa. Data points from isotherms conducted at different temperatures (b – e) H_2 and D_2 isotherms at temperatures of 195, 178. 159 and 143 K respectively. Isotherm graphs include full adsorption isotherm and partial desorption isotherm.

As it can be seen from Figure 7, at temperatures above 195 K, the uptake of H_2 and D_2 is almost the same showing negligible selectivity. As the temperature is reduced from 273 K, adsorption uptake initially increases exponentially, but between 195 K and 143 K, the adsorption begins to be blocked and reaches a maximum at 159 K. Between 159 K and 143 K, the adsorption capacity at 100 kPa of H_2 decreases from 0.311 mmol/g to 0.194 mmol/g (38% reduction), while for D_2 it decreases from 0.456 mmol/g to 0.355 mmol/g (22% reduction). This reduction in adsorption as the temperature is reduced from 159 K to 143 K, suggests the potassium cations in the K-CHA are starting to block access of H_2 and D_2 molecules to the pores. The results show that between 143 – 178 K, H_2 adsorption is blocked more strongly than D_2, leading to an exponential increase in D_2/H_2 selectivity. The ideal D_2/H_2 selectivity (measured at 100 kPa) rises significantly as the adsorption temperature is reduced, rising from 1.1 at 195 K to a maximum D_2/H_2 selectivity of 1.83 at 143 K. This is a remarkably high D_2/H_2 selectivity for an adsorbent at such a relatively mild temperature. Most adsorbents must be cooled to 77 K or below to achieve similar D_2/H_2 selectivity [20]. The isotherm data suggests that K-CHA could be operated using pressure-driven desorption, with the working

Another important observation from Figure 7(b-e) is that as the temperature is reduced below 159 K (the critical admission temperature for H_2) the partial desorption isotherm no longer follows the same path as the adsorption isotherm. This adsorption hysteresis is not generally observed for microporous adsorbents like CHA since the standard theory of condensation does not occur in micropores [21]. At higher temperatures (195 – 178 K) the adsorption/desorption difference becomes negligible which suggests it is linked to the critical admission temperature and therefore evidence of the trapdoor effect in CHA. The hysteresis in CHA is likely caused by the energy loss caused as the gas molecules displace the trapdoor cations. From the literature there are no comparative studies that report hysteresis in the isotherms for CHA. Lozinska *et al.* [22] reported hysteresis in Zeolite Rho from CO_2 isotherms and they related this to the cation occupancy in the window positions (trapdoor type effect) [10].

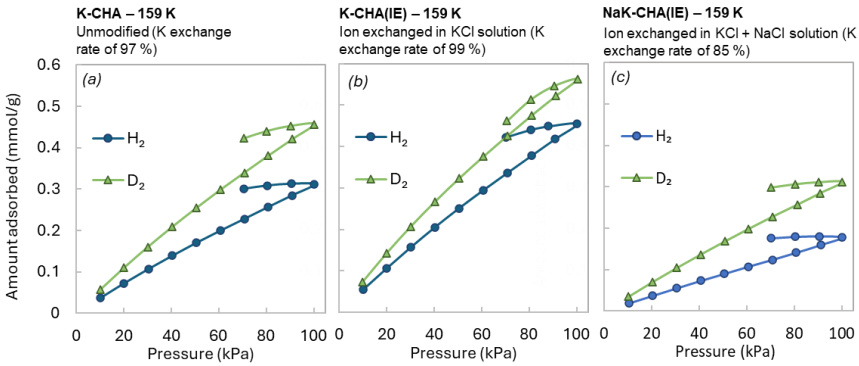

Figure 8 - H_2 and D_2 isotherms at 159 K for CHA with and without ion exchange. Despite minor changes in cation composition, ion exchange treatment increased H_2 uptake by 50 % and reduced D_2/H_2 selectivity. Using mixed Na and K ion exchange, the D_2/H_2 selectivity could be increased. This was important for the breakthrough experiments, since the K-CHA had to be exposed to water during pellet extrusion, it was decided to ion exchange the pellets to NaK-CHA, since this had the best performance.

It was found that post-synthesis treatment of the K-CHA could significantly alter H_2 and D_2 adsorption. Ion exchange treatment of K-CHA in 1 M KCl solution increases the K exchange rate from 97 % to >99 %. However, despite this seemingly minor change in cation content, it was found from conducting isotherms at 159 K that this treatment caused H_2 uptake to increase by 50 % and reduced the D_2/H_2 selectivity from 1.49 to 1.18 (see supporting information). A similar effect was also observed, when treating the K-CHA with other K salt solutions and deionised water. It is thought this is caused by a change in the acid properties of the K-CHA, since the CHA is formed in strongly alkaline KOH. Ion exchange treatment of K-CHA using mixed K and Na salts caused the D_2/H_2 selectivity at 159 K to increase from 1.49 to 1.75 (see supporting information).

3.3 Zeolite 5A H_2/D_2 Isotherms at 143 – 195 K

The H_2 and D_2 adsorption uptake and selectivity of zeolite 5A was measured using isotherm temperatures between 143 – 195 K and the results are shown in Figure 8. Zeolite 5A has cage aperture of 0.5 nm, and so the channels are freely accessible for adsorption of H_2 and D_2 molecules (0.29 nm).

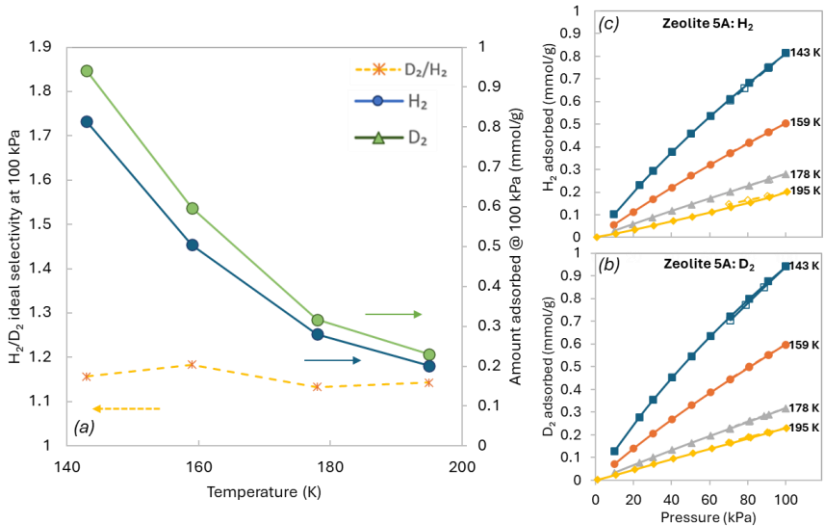

Figure 9: Effect of temperature on H_2 and D_2 adsorption and D_2/H_2 ideal selectivity of zeolite 5A at 100 kPa. Data points from isotherms conducted at different temperatures.

From Figure 8, the amount of H_2 and D_2 adsorbed exponentially increases with lower temperatures which is the typical trend for exothermic physisorption. This is in contrast to K-CHA which contains trapdoor cations which block adsorption at lower temperatures. It can be seen that the D_2/H_2 selectivity of zeolite 5A is very low at 1.14 – 1.18. Unlike K-CHA, the isotherms show no hysteresis.

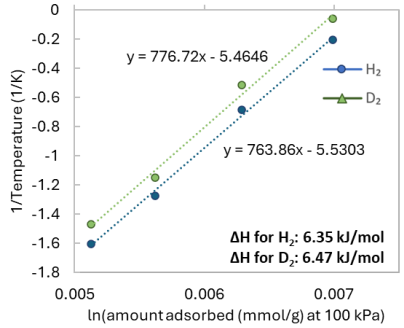

Figure 10: Van't Hoff plot for H_2 and D_2 adsorption on zeolite 5A

The data fits well to a linear Van't Hoff plot (see Figure 9) from which the heat of adsorption was calculated as 6.35 kJ/mol for H_2 and 6.47 kJ/mol for D_2 on zeolite 5A. This low heat of adsorption is typical for the weak hydrogen interaction with zeolite channels (4 – 7 kJ/mol for H_2 [23]).

3.4 Zeolite 3A H_2/D_2 isotherms at 143 – 195 K

The uptake and D_2/H_2 selectivity of zeolite 3A between 143 – 195 K at 100 kPa evaluated from isotherm results are shown in Figure 10. Zeolite 3A has the same framework structure as zeolite

5A, but the pore aperture is restricted by the presence of K^+ cations. The effective pore aperture is reported to be approximately 0.3 nm which is very close to the size of hydrogen molecules [12].

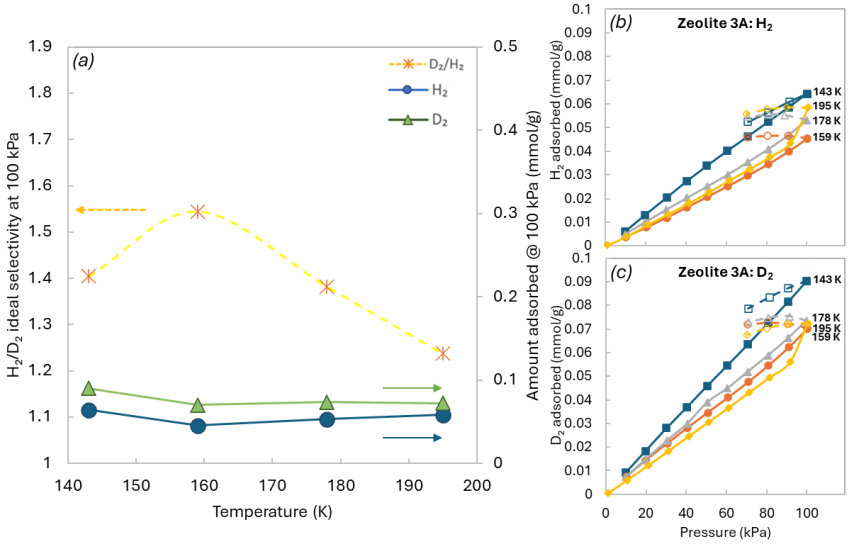

Figure 11: Zeolite 3A H_2 and D_2 isotherm results conducted at temperatures between 143 - 195 K. (a) D_2/H_2 selectivity and uptake at 100 kPa against temperature; (b) H_2 isotherms; (c) D_2 isotherms.

Zeolite 3A had low uptake of H_2 and D_2 over the whole temperature range. Maximum D_2 uptake at 143 K was 0.0904 mmol/g which is only about 10% of the uptake compared to zeolite 5A. This compares to maximum uptake of around 0.01 mmol/g and selectivity of 1.4 for the same material at 170 K [24].

The ideal D_2/H_2 selectivity for zeolite 3A reaches a maximum of 1.54 at 159 K. In comparison, zeolite 5A has an ideal D_2/H_2 selectivity of only 1.18 at 159 K. The higher selectivity of zeolite 3A suggests the K^+ cations in zeolite 3A are able to selectively block H_2 compared to D_2. It is thought that the K^+ cations in the zeolite A framework effectively narrow the pore aperture, causing high resistance to diffusion of gas molecules larger than 0.3 nm [12]. However, H_2 and D_2 have almost identical molecular size and so this would not lead to the observed selectivity. Furthermore, H_2 tends to diffuse faster than D_2 and so this model would produce the opposite isotope selectivity to the one observed. The observed high D_2/H_2 selectivity suggests that a similar trapdoor mechanism could be at work to that seen with K-CHA. Zeolite 3A contains K^+ cations in the pore apertures, a feature shared with the trapdoor chabazite. Furthermore, the D_2/H_2 selectivity of these two adsorbents is remarkably similar, with maximum selectivity occurring in a similar temperature range. This hypothesis of trapdoor behaviour is further supported by the observation of hysteresis in the zeolite 3A isotherms that is not present for zeolite 5A. It is suggested that the displacement of the K^+ cations in both K-CHA and zeolite 3A is the key mechanism that enables H_2 and D_2 molecules to adsorb.

3.5 77 K H_2/D_2 isotherms – MOF-74(Ni), zeolite 5A and HKUST-1

At the low temperature of 77 K, H_2 and D_2 are able to interact strongly with microporous surfaces and reach relatively moderate surface coverages even with a low heat of adsorption. Therefore, H_2 and D_2 isotherms measured at 77 K follow a Langmuir monolayer type relation.

H_2 and D_2 isotherms were measured at 77 K for MOF-74(Ni), HKUST-1 and zeolite 5A. The ideal D_2/H_2 selectivity was calculated using Ideal Adsorbed Solution Theory (IAST) for a theoretical 50:50 H_2/D_2 mixture. The isotherm results are shown in linear and logarithmic plots in Figures 11(a) and 11(b) respectively. The IAST selectivity is shown in Figure 11(c).

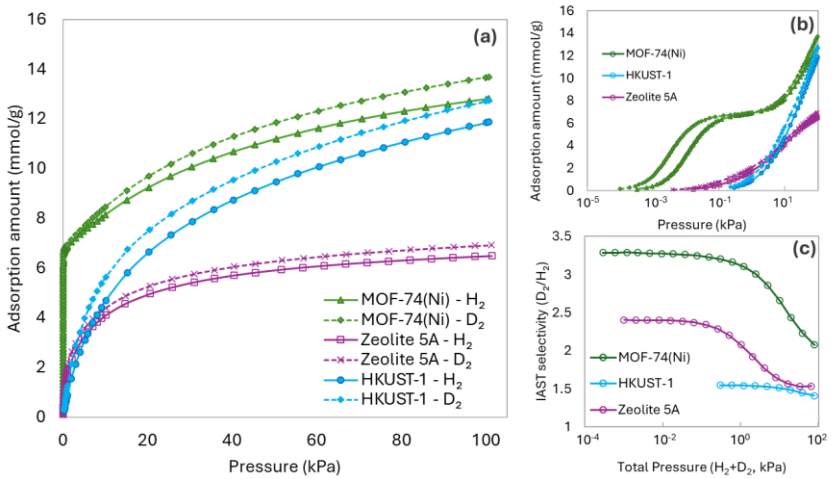

Figure 12: H_2 and D_2 isotherm results for adsorbents tested at 77 K (MOF-74(Ni), zeolite 5A, HKUST-1). (a) Linear isotherm plots; (b) logarithmic isotherm plots; (c) Ideal D_2/H_2 selectivity calculated using IAST model.

The linear isotherm plot in Figure 11 shows that MOF-74(Ni) adsorbs significant amounts of H_2 and D_2 at extremely low pressures. This is quite uncommon for H_2 at 77 K, and is caused by Ni(II) open metal sites in MOF-74(Ni) which have a very high heat of adsorption for H_2 and D_2 [25]. From the log plot, adsorption begins at around $1x10^{-3}$ kPa. There are a limited number of open metal sites and once these become saturated, any further H_2 adsorption occurs at much weaker binding sites. The log plot shows that D_2 adsorption occurs at lower pressures than H_2, suggesting a higher affinity of the open metal sites for D_2. The IAST model results estimates a D_2/H_2 selectivity of 3.3 and lower pressures which reduces to 2.1 at higher pressures.

Compared to MOF-74(Ni), it is clear from the isotherm shape that HKUST-1 does not contain open metal sites that can strongly interact with H_2 and D_2. HKUST-1 contains Cu(II) open metal sites which have been shown to have a strong interaction with other gases (CO_2 and CH_4) [26-28] but from these results it appears that they have a low affinity for H_2. Although HKUST-1 has a weak interaction with H_2, it has very high BET surface area measured to be between 1663 – 2045 m^2/g (see supporting information), and this means that at higher pressures (100 kPa), HKUST-1 can adsorb significant amounts of H_2. However, the D_2/H_2 selectivity is much lower than the other adsorbents tested.

Zeolite 5A contains Ca^{2+} cations which can act as adsorption sites for H_2 and D_2. The 77 K isotherms in Figure 11 show that zeolite 5A can adsorb H_2 and D_2 at low pressures (0.01 – 0.1 kPa), with an IAST D_2/H_2 selectivity of 2.4 at 77 K. This is a similar finding to the study by Giraudet *et al.* [29] who found the presence of +2 charge cations such as Ca^{2+} and Mg^{2+} in zeolite X significantly increased D_2/H_2 selectivity. The IAST model shows high D_2/H_2 selectivity of 2.4 at low pressures (10^{-3} – 10^{-1} kPa) but at about 2 kPa, the selectivity drops to 1.52. At low pressures, H_2 and D_2 essentially only adsorb to the high affinity Ca^{2+} sites which have high D_2/H_2 selectivity. At higher pressures, these sites become saturated, and adsorption also occurs on the lower affinity sites, driven by the higher pressures. Since these adsorption sites have lower selectivity, this causes the overall selectivity to drop at higher pressures.

The results show that at 77 K, high affinity adsorption sites such as those present in zeolite 5A and MOF-74(Ni) can achieve high D_2/H_2 selectivity. These low temperature adsorbents also can achieve relatively high D_2 uptake compared to the high temperature isotherms conducted at 143 – 195 K. However, high selectivity is only achievable at low pressures (< 1 kPa), since at higher pressures, adsorption to weaker affinity sites significantly reduces the selectivity. These low-pressure adsorption conditions would likely be impractical for large scale separation units considering the vacuum pumps required to re-pressurise the product gases. The low pressure will severely reduce desorption rate in large columns, since the column pressure drop can approach the total pressure in the system. Due to the high affinity for hydrogen isotopes, these adsorbents most likely would require regeneration by heating the column to higher temperatures to initiate desorption. Temperature changes can be very slow especially for large columns, and are highly energy intensive, especially at these extreme cryogenic temperatures.

In comparison, the isotherm data for K-CHA and NaK-CHA at 143 K and 159 K, suggest trapdoor chabazite could be pressure regenerated by cycling between 10 – 100 kPa, with very little drop in working capacity or selectivity. Note that the D_2/H_2 ideal selectivity of K-CHA of 1.83 K at 143 K, was calculated at 100 kPa but rises to 2.26 at 10 kPa. This high D_2/H_2 selectivity of trapdoor chabazite over a practical operating pressure regime, make it the most suitable adsorbent tested so far for large scale isotope separation using energy efficient pressure-swing operation.

3.6 H_2/D_2 breakthrough testing using whistle gas density sensor

Breakthrough testing was conducted under dynamic flow conditions using a D_2/H_2 binary gas mixture. All adsorbents were tested using two different breakthrough methodologies to compare the kinetics of displacement and competitive D_2/H_2 adsorption. The first is displacement breakthrough, similar to the experiment conducted by Kotoh et al. [30] in which adsorbed H_2 is displaced by D_2 in the test gas. The second experiment is a novel adaption to the standard frontal breakthrough which was designed specifically to test H_2/D_2 under PSA relevant conditions. Instead of using an inert carrier gas as in previous literature studies [18, 31, 32], adsorption of the D_2/H_2 test gas occurs from vacuum pressure. The test gas is fed into the column with the outlet valve closed which causes the pressure to rise. Once the column reaches atmospheric pressure, the column outlet is opened, allowing the depleted gas to exit. Similar frontal tests have been conducted before on Pd columns [33], but this is the first time it has been applied to adsorbents for H_2/D_2 separation. In this methodology the frontal breakthrough curves will be truncated if the adsorbent has a low selectivity. This is because the D_2 can reach the column outlet before the H_2 has fully pressurised the outlet. The experimental operation is very similar to an actual vacuum pressure swing adsorption column and so the separation performance should approximate well with that achievable for gas separation applications at larger scales.

NaK-CHA were used for breakthrough tests instead of K-CHA because they exhibited the best D_2/H_2 ideal separation as determined from isotherm data. Zeolite 5A was tested at both 159 K and 77 K. The displacement and frontal breakthrough results for NaK-CHA at 159 K and Zeolite 5A at 77 K and 159 K are shown in Figure 12. In all cases, we see that the breakthrough time reduces as the flow rate is increased as would be expected.

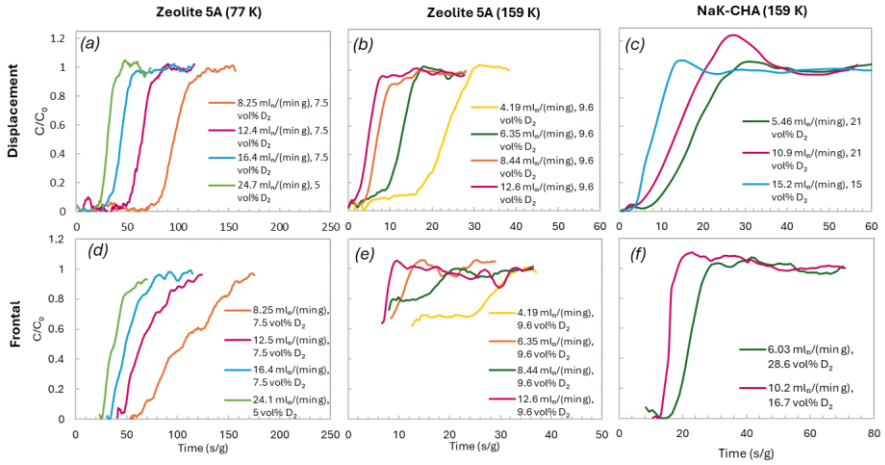

Figure 13 – Mixed H_2/D_2 breakthrough results showing displacement breakthrough results in (a – c) and frontal breakthrough results in (d – f). Results for zeolite 5A at 77 K, zeolite 5A at 159 K and NaK-CHA at 159 K are shown in (a & d), (b & e) and (c & f) respectively. Flow rates as shown in the legend have been standardised against the adsorbent mass. The frontal breakthrough for zeolite 5A at 159 K (shown in (e)) has a non-ideal breakthrough curve profile with the curve beginning above $C/C_0 = 0.6$. This shows that the column is unable to fully separate the D_2/H_2 mixture. An overshoot (roll up effect) is observed for NaK-CHA in (c & f).

The whistle gas density sensor is shown to capture the shape of the breakthrough curve in each case. While there is some random noise in the signal, which is sensitive to flow disturbances, this has a minimal impact on the finding of approximate breakthrough time and the calculation of uptake which is calculated from the integral area.

Zeolite 5A at 77 K has the longest breakthrough times due to the higher uptake of this adsorbent at this temperature. This is despite the higher flow rates of 8.25 – 24.7 $ml_n/(min\ g)$ were used in these tests compared to 4.19 – 12.6 $ml_n/(min\ g)$ for the other tests. For the displacement breakthrough (Figure 12(a)) a typical symmetrical curve is produced close to an ideal normal distribution. For the frontal (Figure 12(d)), the beginning of the curve is truncated. As previously explained, this is caused by the low D_2/H_2 selectivity which means the D_2 begins to reach the outlet before it has reached atmospheric pressure.

For zeolite 5A at 159 K, the breakthrough time is much shorter than at 77 K indicating lower uptake. The frontal breakthrough curves show that the adsorbent column was unable to fully separate the D_2/H_2 mixture, as shown by breakthrough starting at $C/C_0 = 0.6$. This shows that the zeolite 5A column at 159 K was not able to fully separate the H_2/D_2 mixture due to the low separation efficiency of zeolite 5A at this temperature. Compared to the displacement experiment, the frontal breakthrough curves exhibit a longer time period between initial breakthrough and equilibrium breakthrough which is also observed to a lesser extent for the 77

K zeolite 5A results. This displacement breakthrough curves exhibit a self-sharpening mechanism, since any D_2 adsorbed will displace an H_2 molecule, and this effectively doubles the concentration gradient caused by adsorption. In frontal breakthrough, D_2 adsorption can occur through displacement, but also competitive adsorption where H_2 is adsorbing alongside D_2. This reduces the concentration gradient caused by D_2 adsorption and is more important when the selectivity is low, as is the case for zeolite 5A at 159 K.

For NaK-CHA at 159 K, displacement breakthrough, shown in Figure 12(c), occurs quickly due to the low uptake of this adsorbent. The frontal breakthrough curve starts at $C/C_0 = 0$ showing that D_2 is being selectivity adsorbed leaving pure H_2 in the outlet gas stream. These results confirm the ability of the trapdoor effect in NaK-CHA to separate mixtures of hydrogen isotopes at relatively mild cryogenic temperatures. This is in contrast to zeolite 5A which at the same temperature of 159 K, was unable to fully separate the D_2/H_2 mixture. For NaK-CHA at 159 K, a longer time period between initial breakthrough and equilibrium breakthrough occurs for the displacement breakthrough rather than the frontal experiments, which is the opposite to the two temperature tests for zeolite 5A. For NaK-CHA, the movement of gas molecules through the zeolite pores is restricted by the trapdoor cations. In displacement breakthrough, the H_2 molecules must leave the zeolite pores for D_2 to adsorb, however the trapdoor mechanism selectively blocks H_2. Hence this limits the D_2 uptake rate in the displacement experiment, when compared to the frontal experiment. The NaK-CHA breakthrough curves appear to show a roll up effect where the deuterium concentration rises above C_0. Roll up effects are normally caused by a strong adsorbing species which displace a weaker adsorbed species [34], or a difference in the adsorption kinetics between H_2 and D_2.

The results for the mean D_2 uptake for both the displacement and frontal experiments are calculated and shown in Table 2. To account for differences in D_2 concentration used in the experiments, the D_2 uptake was standardised to 9.6 vol% D_2, assuming D_2 uptake is proportional to the D_2 concentration given the small experimental concentration range.

Table 2: Mean D_2 uptake from displacement and frontal breakthrough experiments. Since the D_2 concentration varied between experiments, assuming uptake is proportional to D_2 concentration, in the short concentration range the uptake values have all been standardised at 9.6 vol% D_2.

Adsorbent	**Temp (K)**	**Standardized D_2 uptake (mmol/g)**		**% difference in D_2 uptake (frontal – displacement)**
		Displacement	**Frontal**	
Zeolite 5A	77	0.770	0.961	20 %
	159	0.0612	0.0663	8 %
NaK-CHA	159	0.0159	0.0524	70 %

From Table 2 it can be seen that D_2 uptake from displacement breakthrough is always lower than frontal breakthrough for both zeolite 5A and NaK-CHA. In displacement breakthrough, D_2 must first displace H_2 before it can adsorb, and this creates a kinetic barrier that inhibits adsorption. For frontal displacement, since there is no inhibiting effect, the adsorption amount is close to the equilibrium amount measured from isotherms (see table 3). Also from Table 2, it can be seen that for zeolite 5A the difference in uptake is more significant at lower temperatures suggesting H_2 molecules inhibit D_2 more at lower temperature. This is similar finding to other authors who found lower temperatures made it more difficult for D_2 to displace H_2 because of the higher heat of adsorption. Fitzgerald et al. [18] found that displacement of H_2 by D_2 on Cu(I)-

MFU-4l took much longer as the temperature was reduced from 185 K to 77 K, since H_2 would remain bound to strongly adsorbing sites. The heat of adsorption as measured in section 3.3 for zeolite 5A at 6.35 kJ/mol for H_2 is much lower than Cu(I)-MFU-4l at 32 kJ/mol [18] and so the kinetic hinderance is much less. Bezverkhyy et al. [9] also found adsorption of H_2 and D_2 on Na-CHA and Ca-CHA at took much longer to reach higher D_2/H_2 as the temperature was reduced from 77 K to 38 K.

The adsorbent with the most significant difference in uptake between frontal and displacement breakthrough at any temperature is NaK-CHA at 159 K. Displacement breakthrough uptake for NaK-CHA is 70 % less than for frontal breakthrough. For NaK-CHA, H_2 and D_2 can only adsorb to weakly bound sites such as the aluminosilicate cage or K^+ cations [29], and the higher temperature of 159 K also helps to reduce the kinetic barrier of the energy wells created by adsorption sites. Instead, the main resistance to H_2 displacement in NaK-CHA is likely to be the trapdoor effect which selectively blocks H_2. In the case of displacement breakthrough experiments, the H_2 molecules must first exit through the CHA trapdoor cations before D_2 can adsorb. Since H_2 molecules cannot diffuse out through the trapdoor quickly enough, this prevents D_2 from diffusing in and adsorbing. In frontal breakthrough, the D_2 can interact with the trapdoor cation without the need for H_2 to exit from the chabazite pores. This allows the D_2 molecules to pass more freely through the trapdoor windows, leading to higher uptake.

Table 3 presents the averaged uptake and separation factor from the frontal breakthrough experiments for the various sorbents and compared to the uptake from the adsorption isotherm experiments in section 3.2 – 3.5. In all cases, the uptake from the frontal breakthrough experiments are between 5 – 14 % greater than the isotherm uptake. It is thought this small difference follows from experimental error in the breakthrough experiment and reflects the challenge of breakthrough experimentation with hydrogen isotopologues given their low uptake. The D_2/H_2 separation factor, as measured from the frontal breakthrough data, has good agreement with the ideal selectivity determined from single gas isotherm experiments using the IAST theory. The zeolite 5A data at 77 K is in good agreement with literature data tested under similar conditions. Kotoh *et al.* tested zeolite 5A at 77 K under mixed isotope conditions [35] and reported a separation factor of 2.0 at 1 bar. This agreement with the literature and isotherm data helps to confirm the effectiveness of the frontal breakthrough method in measuring the D_2/H_2 selectivity. For zeolite 5A at 159 K, the average D_2/H_2 separation factor is 1.25 which is close to the ideal selectivity value of 1.18 determined from the isotherm measurements.

Table 3: Summary of uptake and D_2/H_2 selectivity as measured by frontal breakthrough results for NaK-CHA at 159 K and zeolite 5A at both 77 K and 159 K and compared to results from isotherm data. For the purposes of comparison, the Isotherm uptake data are adjusted by 15% to account for 15 wt.% inert clay in NaK-CHA and zeolite 5A pellets used in breakthrough results.

Material	Temp (K)	Mean total H_2 & D_2 uptake (mmol/g)		Mean D_2/H_2 selectivity *	
		Frontal	Isotherm	Frontal	Isotherm
Zeolite 5A	77	6.2 ± 0.69	5.90 *	1.7 ± 0.19	1.53
	159	0.58 ± 0.14	0.507 *	1.25 ± 0.24	1.18
NaK-CHA	159	0.286 ± 0.030	0.265 *	2.71 ± 0.70	1.75

**actual separation factor and ideal selectivity from isotherm data.*

There is a difference between the single gas prediction of selectivity, and the actual dynamic measurement for NaK-CHA. For NaK-CHA at 159 K, an average D_2/H_2 separation factor of 2.71± 0.70 was calculated from the frontal breakthrough results. This is significantly higher than the D_2/H_2 selectivity of 1.75 predicted by the isotherm data suggesting that the selectivity of NaK-CHA is greater under dynamic mixed gas conditions is higher than predicted from the individual isotherm data. Under mixed gas conditions, and for unrestricted channels, the D_2 and H_2 molecules must compete for limited adsorption sites, and this can increase selectivity. This phenomenon cannot be observed during single gas isotherm experiments and this explains the difference in selectivity in zeolites [34]. In CHA, it is thought that the observed increase in selectivity during the frontal experiment is due to the competitive interaction of H_2 and D_2 with the trapdoor cation which can either block or enable passage of the gas molecules. This finding is highly significant for adsorption processes for this application, because it means that separation factors in practice will exceed those determined by single gas isotherms. These are the first measurements of the dynamic adsorption of gas molecules through the trapdoor effect and shows how the mechanism operates under conditions relevant for industrial gas separation applications.

Commented [RB1]: Paragraph title sentence needed, I've suggested this but feel free to change it

4. Conclusion

Trapdoor chabazite was shown to have a high hydrogen isotope selectivity at temperatures much higher than other adsorbents using both single gas isotherms and mixed gas breakthrough tests. A trapdoor mechanism in zeolite 3A is also reported for the first time. The ideal D_2/H_2 selectivity of K-CHA is highly temperature sensitive, with almost no selectivity at 195 K, but rising to 1.75 at 143 K as the critical admission temperature is reached and H_2 starts to be blocked. A hysteresis effect is reported in trapdoor chabazite for the first time which only occurs between 143 – 178 K. The favourable adsorption equilibria of trapdoor chabazite suggest that pressure-driven desorption could be used enabling the adsorbent to be rapidly cycled even in large scale applications.

A bespoke breakthrough setup using a novel online whistle gas density sensor was successfully used to test dynamic H_2/D_2 adsorption in NaK-CHA at 159 K and zeolite 5A at 77 K and 159 K. The detection system was able to replace more complex mass spectroscopy and achieve real-time isotope measurements in an inexpensive setup. Using the breakthrough apparatus, the D_2/H_2 separation factor of NaK-CHA was measured under mixed gas flow conditions to be approximately 2.71 ± 0.70 at 159 K, 1 bar. Displacement of H_2 by D_2 is significantly inhibited by the slow diffusion of H_2 through the trapdoor window.

These results demonstrate that high hydrogen isotope selectivity are achievable at practical mild cryogenic temperatures in trapdoor adsorbents. Trapdoor chabazite has the potential for efficient large scale isotope separation with low tritium inventory, addressing one of the key challenges facing the realisation of commercial fusion plants.

[1] World_Nuclear_Association. Nuclear Fusion Power [Internet]. 2020 [cited 04/01/21]. Available from: https://www.world-nuclear.org/information-library/current-and-future-generation/nuclear-fusion-power.aspx].

[2] Chapman IT, Morris AW. UKAEA capabilities to address the challenges on the path to delivering fusion power. *Philos Trans A Math Phys Eng Sci*. 2019;377(2141):20170436-.
[3] Lawless R, Butler B, Hollingsworth A, Camp P, Shaw R. Tritium Plant Technology Development for a DEMO Power Plant. *Fusion Science and Technology*. 2017;71(4):679-86.
[4] Shaw RCR, Butler B. Applicability of a cryogenic distillation system for D-T isotope rebalancing and protium removal in a DEMO power plant. *Fusion Engineering and Design*. 2019;141:59-67.
[5] Day C, Battes K, Butler B, Davies S, Farina L, Frattolillo A, George R, Giegerich T, Hanke S, Härtl T, Igitkhanov Y, Jackson T, Jayasekera N, Kathage Y, Lang PT, Lawless R, Luo X, Neugebauer C, Ploeckl B, Santucci A, Schwenzer J, Teichmann T, Tijssen T, Tosti S, Varoutis S, Cortes AV. The pre-concept design of the DEMO tritium, matter injection and vacuum systems. *Fusion Engineering and Design*. 2022;179:113139.
[6] Bainbridge N, Bell AC, Brennan PD, Knipe S, Lässer R, Stagg R. Operational experience with the JET AGHS cryodistillation system during and after DTE1. *Fusion Engineering and Design*. 1999;47(2):321-32.
[7] Roder HM, Childs GE, McCarty RD, Angerhofer PE. Survey of the Properties of the Hydrogen Isotopes Below Their Critical Temperatures. United States. National Bureau of Standards.; 1973.
[8] Weinrauch I, Savchenko I, Denysenko D, Souliou SM, Kim HH, Le Tacon M, Daemen LL, Cheng Y, Mavrandonakis A, Ramirez-Cuesta AJ, Volkmer D, Schütz G, Hirscher M, Heine T. Capture of heavy hydrogen isotopes in a metal-organic framework with active Cu(I) sites. *Nature Communications*. 2017;8(1):14496.
[9] Bezverkhyy I, Boyer V, Cabaud C, Bellat J-P. High Efficiency of Na- and Ca-Exchanged Chabazites in D2/H2 Separation by Quantum Sieving. *ACS Applied Materials & Interfaces*. 2022;14(47):52738-44.
[10] Shang J, Li G, Webley PA, Liu JZ. A density functional theory study for the adsorption of various gases on a caesium-exchanged trapdoor chabazite. *Computational Materials Science*. 2016;122:307-13.
[11] Shang J, Li G, Singh R, Gu Q, Nairn KM, Bastow TJ, Medhekar N, Doherty CM, Hill AJ, Liu JZ, Webley PA. Discriminative Separation of Gases by a "Molecular Trapdoor" Mechanism in Chabazite Zeolites. *Journal of the American Chemical Society*. 2012;134(46):19246-53.
[12] Kulprathipanja S. Zeolites in Industrial Separation and Catalysis: John Wiley & Sons; 2010.
[13] Li G, Shang J, Gu Q, Awati RV, Jensen N, Grant A, Zhang X, Sholl DS, Liu JZ, Webley PA, May EF. Temperature-regulated guest admission and release in microporous materials. *Nature Communications*. 2017;8(1):15777.
[14] Lin C-H, Lin C-H, Li Y-S, He Y-S. Development and Application of a Milli-Whistle for Use in Gas Chromatography Detection. *Anal Chem*. 2010;82(17):7467-71.
[15] Walker RJ. Sonic Standing Wave Gas Density Monitor. In: Fast RW, editor. Advances in Cryogenic Engineering. Boston, MA: Springer US; 1988. p. 1081-7.
[16] Reed. Introduction to Energy Dispersive X-ray Spectrometry (EDS) [Internet]. 1995 [Available from: https://cfamm.ucr.edu/media/126/download?attachment].
[17] Rouquerol J, Rouquerol F, Sing K. Adsorption by Powders and Porous Solids : Principles, Methodology and Applications. San Diego, UNITED KINGDOM: Elsevier Science & Technology; 1998.
[18] FitzGerald SA, Mukasa D, Rigdon KH, Zhang N, Barnett BR. Hydrogen Isotope Separation within the Metal–Organic Framework Cu(I)-MFU-4l. *The Journal of Physical Chemistry C*. 2019;123(50):30427-33.
[19] Baerlocher C, McCusker LB. Database of Zeolite Structures [Internet]. 2017 [cited 09/09/2023]. Available from: http://www.iza-structure.org/databases/].

[20] Beenakker JJM, Borman VD, Krylov SY. Molecular transport in subnanometer pores: zero-point energy, reduced dimensionality and quantum sieving. *Chemical Physics Letters*. 1995;232(4):379-82.
[21] Donohue MD, Aranovich GL. Adsorption Hysteresis in Porous Solids. *Journal of Colloid and Interface Science*. 1998;205(1):121-30.
[22] Lozinska MM, Mangano E, Mowat JPS, Shepherd AM, Howe RF, Thompson SP, Parker JE, Brandani S, Wright PA. Understanding Carbon Dioxide Adsorption on Univalent Cation Forms of the Flexible Zeolite Rho at Conditions Relevant to Carbon Capture from Flue Gases. *Journal of the American Chemical Society*. 2012;134(42):17628-42.
[23] Knight EW, Gillespie AK, Prosniewski MJ, Stalla D, Dohnke E, Rash TA, Pfeifer P, Wexler C. Determination of the enthalpy of adsorption of hydrogen in activated carbon at room temperature. *International Journal of Hydrogen Energy*. 2020;45(31):15541-52.
[24] Kotoh K, Kimura K, Nakamura Y, Kudo K. Hydrogen Isotope Separation Using Molecular Sieve of Synthetic Zeolite 3A. *Fusion Science and Technology*. 2008;54(2):419-22.
[25] FitzGerald SA, Burkholder B, Friedman M, Hopkins JB, Pierce CJ, Schloss JM, Thompson B, Rowsell JL. Metal-specific interactions of H2 adsorbed within isostructural metal-organic frameworks. *Journal of the American Chemical Society*. 2011;133(50):20310-8.
[26] Chong KC, Lai SO, Mah SK, Thiam HS, Chong WC, Shuit SH, Lee SS, Chong WE. A Review of HKUST-1 Metal-Organic Frameworks in Gas Adsorption. *IOP Conference Series: Earth and Environmental Science*. 2023;1135(1):012030.
[27] Moellmer J, Moeller A, Dreisbach F, Glaeser R, Staudt R. High pressure adsorption of hydrogen, nitrogen, carbon dioxide and methane on the metal–organic framework HKUST-1. *Microporous and Mesoporous Materials*. 2011;138(1):140-8.
[28] Liu J, Culp JT, Natesakhawat S, Bockrath BC, Zande B, Sankar SG, Garberoglio G, Johnson JK. Experimental and Theoretical Studies of Gas Adsorption in Cu3(BTC)2: An Effective Activation Procedure. *The Journal of Physical Chemistry C*. 2007;111(26):9305-13.
[29] Giraudet M, Bezverkhyy I, Weber G, Dirand C, Macaud M, Bellat J-P. D2/H2 adsorption selectivity on FAU zeolites at 77.4 K: Influence of Si/Al ratio and cationic composition. *Microporous and Mesoporous Materials*. 2018;270:211-9.
[30] Kotoh K, Moriyama S-t, Takashima S, Takahashi K. Breakthrough curves of non-trace H2–D2 mixture replacement adsorption with SZ-13X packed column at 77.4K. *Fusion Engineering and Design*. 2013;88(9):2223-7.
[31] Wu F, Li L, Tan Y, El-Sayed E-SM, Yuan D. The competitive and synergistic effect between adsorption enthalpy and capacity in D2/H2 separation of M2(m-dobdc) frameworks. *Chinese Chemical Letters*. 2021;32(11):3562-5.
[32] Si Y, He X, Jiang J, Duan Z, Wang W, Yuan D. Highly effective H2/D2 separation in a stable Cu-based metal-organic framework. *Nano Research*. 2021;14(2):518-25.
[33] Fukada S, Fujiwara H. Comparison of chromatographic methods for hydrogen isotope separation by Pd beds. *Journal of Chromatography A*. 2000;898(1):125-31.
[34] Thomas WJ, Crittenden B. Adsorption Technology and Design. Oxford: Buttenworth-Heinemann; 1998.
[35] Kotoh K, Kudo K. Multi-Component Adsorption Behavior of Hydrogen Isotopes on Zeolite 5A and 13X at 77.4 K. *Fusion Science and Technology*. 2005;48(1):148-51.